

Investigations of solutions of Einstein's field equations close to λ -Taub-NUT

Florian Beyer

KTH Matematik
10044 Stockholm
Sweden

E-mail: fbeyer@math.kth.se

Abstract. We present investigations of a class of solutions of Einstein's field equations close to the family of λ -Taub-NUT spacetimes. The studies are done using a numerical code introduced by the author elsewhere. One of the main technical complication is due to the S^3 -topology of the Cauchy surfaces. Complementing these numerical results with heuristic arguments, we are able to yield some first insights into the strong cosmic censorship issue and the conjectures by Belinskii, Khalatnikov and Lifschitz in this class of spacetimes. In particular, the current investigations suggest that strong cosmic censorship holds in this class. We further identify open issues in our current approach and point to future research projects.

PACS numbers: 04.20.Dw, 04.25.dc

1. Introduction

Motivated by the desire to understand the history and fate of our universe, studies of cosmological solutions of Einstein's field equations have a long tradition. Observations indicate that there was a big bang in the distant past, and indeed, the simplest cosmological models, namely the Friedmann solutions for reasonable matter fields, predict such a collapse of spacetime. Now, the question arises whether such curvature singularities occur generically in solutions of Einstein's field equations or only under the strong symmetry assumptions underlying the Friedmann models. This problem was solved, namely due to the Hawking-Penrose singularity theorems [26] we can expect incompleteness of causal geodesics in a wide class of situations. However, the information about the origin of the singular behavior provided by these theorems is very limited. One would expect that curvature singularities develop, as in the Friedmann case, which 'stop' the geodesics. But one was able to find solutions, as the λ -Taub-NUT spacetimes discussed below, where the curvature stays bounded but the spacetime becomes acausal in a well-defined sense. Let us restrict in all our investigations to vacuum with positive cosmological constant λ , in which case Einstein's field equations (EFE) in geometric units $c = 1$ and $G = 1/(8\pi)$ read

$$R_{\mu\nu} = \lambda g_{\mu\nu}, \quad (1)$$

and to four spacetime dimensions. Here, $g_{\mu\nu}$ is a Lorentzian metric of signature $(-, +, +, +)$; $R_{\mu\nu}$ represents the Ricci tensor of $g_{\mu\nu}$. One particularly important prototype solution of these equations is the de-Sitter spacetime [26]. The positive cosmological constant is motivated by current observations [43, 44]. Under these (but actually under much wider) assumptions, the Cauchy problem of EFE is well-posed and leads to the notion of the maximal globally hyperbolic development (MGHD) of a given Cauchy data set. See [2] and references therein for a review of the details. Now, for Cauchy data corresponding to a λ -Taub-NUT spacetime for instance, the corresponding MGHD is extendible in several inequivalent ways as smooth solutions of EFE. In this sense, Einstein's theory has only limited predictive power. The hope, expressed by strong cosmic censorship (SCC) essentially first formulated by Penrose [35, 36], is that, although examples like the λ -Taub-NUT spacetimes exist, the MGHD corresponding to a *generic* Cauchy data set is inextendible. This would rescue the predictive power of Einstein's theory. So far, there is neither a clear idea which topology on the space of initial data is supposed to give rise to the notion of 'genericity' here, nor which class of extensions to choose in general. Although this issue has only been solved successfully so far in special situations, some of which are commented on below, interesting new insights have been obtained as summarized in [2, 39].

Besides strong cosmic censorship there are other open problems of interest for cosmological spacetimes. Belinskii, Khalatnikov, and Lifschitz [30, 5, 6] conjectured, what we nowadays call BKL-conjecture, a description of the properties of solutions with curvature singularities. We give only few further details later, and just remark that it is still a matter of active research whether their conjecture holds generically [2, 39]. Another outstanding problem is to find a characterization of the development of generic cosmological solutions in the expanding time direction, and the notion of cosmic no-hair essentially introduced in [27] is one promising scenario.

In our work, we focus on the class of Gowdy spacetimes with spatial \mathbb{S}^3 -topology which yields one of the main technical complications. In that class, the issue of SCC and the BKL-conjecture is still unsolved; however, there are strong expectations due

to results in the Gowdy case with spatial \mathbb{T}^3 -topology. We restrict to a special class of solutions which obey a generalized notion of cosmic no-hair by construction. Further, this class is close to λ -Taub-NUT in the sense that it incorporates a “perturbation” parameter ε such that $\varepsilon = 0$ corresponds to a λ -Taub-NUT spacetime. Our solutions are constructed using Friedrich’s notion of the \mathcal{I}^+ -Cauchy problem discussed below by means of a numerical code introduced in [9]. The purpose of our investigations is to check whether SCC is true in this class and how the dynamics gives rise to it when ε approaches zero. We are further interested in the BKL-conjecture. We see these investigations in this special class as first steps in order to shed further light on the general SCC and BKL-conjectures.

The paper is organized as follows. First we give the relevant background material in section 2, including some remarks about the conformal field equations and future asymptotically de-Sitter spacetimes, the definition of the λ -Taub-NUT family, a short introduction into the class of Gowdy spacetimes with spatial \mathbb{S}^3 -topology, our family of initial data and a few comments about our numerical method. In section 3, we write our main result, support it by means of numerical computations and heuristic arguments and discuss the current limitations of the approach. Finally we conclude.

2. Background material

2.1. Notations and conventions

In this paper, we will always assume Einstein’s summation convention when we write tensorial expressions. Any tensor can be represented by the abstract symbol, say, T or by abstract index notation, e.g. T^μ_ν , dependent on the context. Note however, that when we write such an indexed object, we can mean either the abstract tensor or a special component with respect to some basis. Hopefully this will be always clear from the context. Our convention is that Greek indices $\mu, \nu, \dots = 0, \dots, 3$ refer to some choice of local spacetime coordinates, whereas Latin indices $i, j, \dots = 0, \dots, 3$ represent indices with respect to some orthonormal frame field. When we have chosen a time coordinate x^0 , then Greek indices $\alpha, \beta, \dots = 1, 2, 3$ represent spatial coordinates, and for a choice of frame $\{e_i\}$ with timelike vector field e_0 , Latin indices $a, b, \dots = 1, 2, 3$ refer to spatial frame indices. Writing $\{e_i\}$ just means the collection of tangent vector fields $\{e_0, \dots, e_3\}$. If a 2-indexed object is written in brackets, for instance (T^μ_ν) , we mean the matrix of its components, where the first index labels the lines of the matrix and the second one the columns.

2.2. Future asymptotically de-Sitter spacetimes and the conformal field equations

Let a smooth Lorentzian manifold $(\tilde{M}, \tilde{g}_{\mu\nu})$ be given; not necessarily a solution of EFE. According to Penrose [34, 36], it is said to have a smooth conformal compactification if there exists a smooth Lorentz manifold-with-boundary (M, g) with boundary $\mathcal{I} := \partial M$ and a smooth function $\Omega : M \rightarrow \mathbb{R}$ such that

- (i) there is a diffeomorphism $\Phi : \tilde{M} \rightarrow M \setminus \mathcal{I}$ such that $\tilde{g} = \Phi_* \left(\Omega^{-2} g|_{M \setminus \mathcal{I}} \right)$,
- (ii) we have $\Omega > 0$ in the interior of M , and, $\Omega = 0$ and $d\Omega \neq 0$ on \mathcal{I} .

For simplicity we will always identify \tilde{M} with $\Phi(\tilde{M}) \subset M$. Under these assumptions, \mathcal{I} is called conformal boundary and can be interpreted as representing “infinity” of the physical spacetime $(\tilde{M}, \tilde{g}_{\mu\nu})$. In the following, quantities which are related to

the physical metric $\tilde{g}_{\mu\nu}$ are marked with a tilde, while those related to the conformal metric $g_{\mu\nu}$ are not marked. For a recent discussion and several examples see [19]. The main prototype solution of EFE with $\lambda > 0$ with a smooth conformal compactification is the de-Sitter solution. Further examples are provided by the λ -Taub-NUT family discussed below. Now, in general if $(\tilde{M}, \tilde{g}_{\mu\nu})$ is a solution of (1) in vacuum with $\lambda > 0$, then the corresponding conformal boundary \mathcal{J} must be spacelike. In this case, we define \mathcal{J}^+ as the intersection of \mathcal{J} with the chronological future of \tilde{M} in M and analogously \mathcal{J}^- . We assume in all what follows that \mathcal{J} is the disjoint union of \mathcal{J}^+ and \mathcal{J}^- , each of which is allowed to be empty so far. If \mathcal{J}^+ is non-empty, we call $(\tilde{M}, \tilde{g}_{\mu\nu})$ future asymptotically de-Sitter (FAdS); in the same way one can define past asymptotically de-Sitter solutions. According to [3], a FAdS spacetime with compact \mathcal{J}^+ is globally hyperbolic if and only if it is future asymptotically simple, i.e. all future directed inextendible null geodesics starting in \tilde{M} have future endpoints on \mathcal{J}^+ . Then, all Cauchy surfaces of $(M, \tilde{g}_{\mu\nu})$ are actually homeomorphic to \mathcal{J}^+ . From the physical point of view it is further important that all FAdS solutions obey a generalized notion of the cosmic no-hair picture [7], and hence provide a model of the current observational predictions for the future of our universe.

In order to compute solutions of the EFE in terms of conformal variables directly, Friedrich succeeded in finding a formulation of EFE called conformal field equations (CFE), which is both conformally invariant and regular even on \mathcal{J} . By conformal invariance we mean that in addition to the coordinate gauge freedom of Einstein's theory, the CFE obey the conformal gauge freedom; i.e. the possibility to conformally rescale the conformal metric with a smooth positive function leaving the physical metric invariant. By 'regular' we mean that these equations provide evolution equations which are hyperbolic even in \mathcal{J} . A review of his results and further references are given in [19]. His formalism is restricted to four spacetime dimensions, the relevant case for our investigations. Anderson [1] was able to find a different formulation applicable in arbitrary even spacetime dimensions. We, however, restrict here to Friedrich's CFE which we write in a special form below. Under the assumptions above, in particular for $\lambda > 0$, the CFE allow one to formulate what we call \mathcal{J}^+ -Cauchy problem [16]; Anderson's generalization of this concept was proposed in [1]. The idea is to prescribe data for the CFE on the hypersurface \mathcal{J}^+ including its manifold structure subject to certain constraints implied by the CFE. These data can be integrated into the past by means of evolution equations implied by the CFE. The \mathcal{J}^+ -Cauchy problem is well-posed and the unique FAdS solution corresponding to a given choice of smooth data on \mathcal{J}^+ is smooth as long as it can be extended into the past. It is remarkable that this Cauchy problem allows us to control the future asymptotics of the solutions explicitly by deciding on the data on \mathcal{J}^+ . Concerning the past behavior, the concepts of MGHs and SCC with respect to data on \mathcal{J}^+ are well defined, however, there is only limited a priori control in the same way as it is the case for the Cauchy problem of EFE. In this paper, we will give no details on how the constraints implied on \mathcal{J}^+ look and say only briefly what the relevant data components are, since we do not want to introduce all the geometric concepts now. Instead we refer to [16, 7] where the details have been carried out. In order to choose a complete set of smooth data on \mathcal{J}^+ , besides certain quantities related to the gauge, it turns out to be sufficient to choose the differentiable manifold structure of \mathcal{J}^+ , which we assume to be the standard one on \mathbb{S}^3 , the induced conformal 3-metric $h_{\alpha\beta}$ and the electric part of the rescaled conformal Weyl tensor $E_{\alpha\beta}$ [19, 20]. From those components the complete data set is fixed in terms of algebraic or differential

relations. The choice of these components is unconstrained except for $E_{\alpha\beta}$ which has to satisfy $D^\alpha E_{\alpha\beta} = 0$. Here D is the Levi-Civita covariant derivative operator of $h_{\alpha\beta}$, and the index in the constraint has been raised by means of $h_{\alpha\beta}$. Below, we mention a special class of solutions of this constraint.

For our purposes, we decided to use the so-called general conformal field equations which are the CFE in conformal Gauß gauge [18, 19]. This fixes the gauge freedom for the coordinates, the conformal factor and a frame which is orthonormal with respect to the conformal metric. In our applications, we specialize the gauge even further to what we call Levi-Civita conformal Gauß gauge [7]. One assumption for that is that the conformal geodesics representing the timelines leave \mathcal{J}^+ orthogonally. In particular this implies that they correspond to physical geodesics up to parametrization [22]. Hence this gauge can be considered as a (standard) Gauß gauge with respect to the conformal (and also the physical) metric up to parametrization. We can expect that this simple choice of gauge can lead to serious problems in the evolution, and in fact, we will discuss problems related to the gauge later. In any case, assuming without loss of generality $\lambda = 3$ and having fixed the residual gauge initial data as described in [7], a hyperbolic reduction of the general conformal field equations in Levi-Civita conformal Gauß gauge is

$$\partial_t e_a^c = -\chi_a^b e_b^c, \quad (2a)$$

$$\partial_t \chi_{ab} = -\chi_a^c \chi_{cb} - \Omega E_{ab} + L_{ab}, \quad (2b)$$

$$\partial_t \Gamma_a^b{}_c = -\chi_a^d \Gamma_d^b{}_c + \Omega B_{ad} \epsilon^b{}_c{}^d, \quad (2c)$$

$$\partial_t L_{ab} = -\partial_t \Omega E_{ab} - \chi_a^c L_{cb}, \quad (2d)$$

$$\partial_t E_{fe} - D_{ec} B_{a(f} \epsilon^{ac}{}_{e)} = -2\chi_c^e E_{fe} + 3\chi_{(e}^c E_{f)c} - \chi_c^b E_b^c g_{ef}, \quad (2e)$$

$$\partial_t B_{fe} + D_{ec} E_{a(f} \epsilon^{ac}{}_{e)} = -2\chi_c^e B_{fe} + 3\chi_{(e}^c B_{f)c} - \chi_c^b B_b^c g_{ef}, \quad (2f)$$

$$\Omega(t) = \frac{1}{2} t (2 - t), \quad (2g)$$

for the unknowns

$$u = (e_a^b, \chi_{ab}, \Gamma_a^b{}_c, L_{ab}, E_{fe}, B_{fe}).$$

Among the unknowns are the spatial components e_a^b – with respect to some reference basis specified below – of a smooth frame field $\{e_i\}$ which is orthonormal with respect to the conformal metric and where, in this special gauge, $e_0 = \partial_t$ is the past directed timelike unit normal of the $t = \text{const}$ -hypersurfaces, the spatial frame components of the second fundamental form χ_{ab} of the $t = \text{const}$ -hypersurfaces with respect to e_0 , the spatial connection coefficients $\Gamma_a^b{}_c$, given by $\Gamma_a^b{}_c e_b = \nabla_{e_a} e_c - \chi_{ac} e_0$ where ∇ is the Levi-Civita covariant derivative operator of the conformal metric, the spatial frame components of the Schouton tensor L_{ab} , which is related to the Ricci tensor of the conformal metric by

$$L_{\mu\nu} = R_{\mu\nu}/2 - g_{\mu\nu} g^{\rho\sigma} R_{\rho\sigma}/12,$$

and the spatial frame components of the electric and magnetic parts of the rescaled conformal Weyl tensor E_{ab} and B_{ab} defined with respect to e_0 . In this special conformal Gauß gauge, the timelike frame field e_0 is hypersurface orthogonal, i.e. χ_{ab} is symmetric. In order to avoid confusions, we point out that the conformal factor Ω is part of the unknowns in Friedrich's formulation of the CFE. However, in the special case of vacuum with $\lambda > 0$, it is possible to integrate its evolution equation in any conformal Gauß gauge explicitly [18] so that it takes the special form (2g) in

our gauge. Hence, if the solution develops a smooth \mathcal{J}^- then it must correspond to the $t = 2$ -hypersurface. The initial hypersurface \mathcal{J}^+ corresponds to $t = 0$, and t increases into the past. We note further that, since E_{ab} and B_{ab} are tracefree, we identify $E_{33} = -E_{11} - E_{22}$; the same for the magnetic part. The evolution equations of E_{ab} and B_{ab} are derived from the Bianchi system [19]. In our gauge, the constraint equations implied by the Bianchi system take the form

$$D_{e_c} E^c_e - \eta^{ab} B_{da} \chi_b^d = 0, \quad D_{e_c} B^c_e + \eta^{ab} E_{da} \chi_b^d = 0, \quad (3)$$

where η is the volume form of the spatial conformal metric with $\eta_{123} = 1$, and indices are shifted by means of the conformal metric. The other constraints of the system above are equally important but are ignored for the presentation here. Further discussions of that evolution system and the quantities involved can be found in the references above.

As the reference basis tangential to the $t = \text{const}$ -hypersurfaces assumed to be \mathbb{S}^3 topologically, we choose frame vector fields $\{Y_a\}$ which are $\text{SU}(2)$ -left invariant and satisfy the commutator relations

$$[Y_a, Y_b] = 2 \sum_{c=1}^3 \eta_{abc} Y_c,$$

where η_{abc} is the totally antisymmetric symbol with $\eta_{123} = 1$. These requirements fix those vector fields uniquely up to the specific choice of realization of the $\text{SU}(2)$ -action on \mathbb{S}^3 and up to certain transformations on the three-dimensional real vector space of $\text{SU}(2)$ -left invariant vector fields. We do not list our choices involved here but rather write the explicit expressions below[‡]. Henceforth we write $e_a = e_a^b Y_b$, and in the Bianchi system (2e) and (2f) and corresponding constraints (3), the orthonormal frame fields are interpreted as linear differential operators whose coefficients are given by e_a^b and by the components of $\{Y_a\}$ in some coordinate system which we fix in a moment.

We finally note how the Kretschmann scalar of the physical metric can be computed in terms of the variables above if the physical metric is a solution of EFE in vacuum with $\lambda > 0$,

$$\tilde{\kappa} = \tilde{R}^{ijkl} \tilde{R}_{ijkl} = 24 \frac{\lambda^2}{9} + 8\Omega^6 \sum_{a,b=1}^3 (|E_{ab}|^2 - |B_{ab}|^2). \quad (4)$$

2.3. λ -Taub-NUT solutions

Consider the function $V : \mathbb{R} \rightarrow \mathbb{R}$ defined by

$$V(\tau) = D_0 \tau^4 + 2(3D_0 - 2)\tau^2 + C_0 \tau + 4 - 3D_0$$

where $(D_0, C_0) \in \mathbb{R}^{>0} \times \mathbb{R}$ are arbitrary parameters. For given (D_0, C_0) , let I be a maximal interval on which $V > 0$. Corresponding to the choice of cosmological constant $\lambda > 0$, parameters (D_0, C_0) and interval I , we define the λ -Taub spacetime [11] as the Lorentz manifold (\tilde{M}, \tilde{g}) with $\tilde{M} = I \times \mathbb{S}^3$ and

$$\begin{aligned} \tilde{g} = \frac{3}{\lambda} D_0 \left[-\frac{1 + \tau^2}{V(\tau)} d\tau^2 + \frac{V(\tau)}{1 + \tau^2} \sigma^3 \otimes \sigma^3 \right. \\ \left. + (1 + \tau^2)(\sigma^1 \otimes \sigma^1 + \sigma^2 \otimes \sigma^2) \right] \end{aligned}$$

[‡] To be more precise we choose $\{Y_a\}$ as the reference frame on the spacetime as follows. Let $\{Y_a\}$ be given as before on one $t = \text{const}$ Cauchy surface. Then we extend the frame to the spacetime, keeping the same symbol $\{Y_a\}$, by means of the conditions $[\partial_t, Y_a] = 0$.

which can be shown to be a solution of $\tilde{R}_{\mu\nu} = \lambda \tilde{g}_{\mu\nu}$. Here, $\{\sigma^a\}$ is the dual of the frame $\{Y_a\}$. Note that for a given choice of (D_0, C_0) there can exist several distinct choices of the interval I and hence several distinct λ -Taub spacetimes.

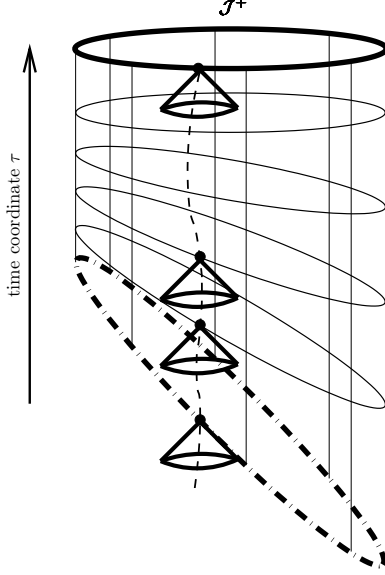


Figure 1. Causal structure of a singular λ -Taub solution.

The λ -Taub spacetimes are globally hyperbolic and maximal with this property. The de-Sitter solution is recovered by choosing the parameters $(D_0, C_0) = (\lambda/3, 0)$, in which case $I = \mathbb{R}$. Indeed, due to the nonlinear stability of the de-Sitter spacetime [17, 1], there is an open neighborhood U of the de-Sitter point in the parameter space $\mathbb{R}^{>0} \times \mathbb{R}$ in which all corresponding λ -Taub spacetimes are causal geodesically complete and asymptotically de-Sitter in the future and in the past. In general, for any given choice of (D_0, C_0) , one can find $\tau_0 \in \mathbb{R} \cup \{-\infty\}$ such that one pick $I =]\tau_0, \infty[$, and we will assume such I in the following. The corresponding λ -Taub solution is FAdS, as depicted in figure 1; note that in our convention ∂_τ is future directed. Now, if V has zeros on \mathbb{R} , i.e. if $\tau_0 \neq -\infty$, we will say that the corresponding λ -Taub spacetime is singular. Indeed, the metric is clearly singular when V becomes zero, however, curvature invariants are bounded. One can show analogously to the case treated in [14] that singular λ -Taub spacetimes are always, independent of the type of zero

of V at τ_0 , extendible and causal geodesically incomplete. In particular, this provides counter examples [8] to theorem 1.3 in [1]. Any extension of a singular λ -Taub solution is non-globally hyperbolic and will be referred to as λ -Taub-NUT. We will not write extensions here but only note the following. The function V can only have a single or double real zero at $\tau = \tau_0$. In both cases the $\tau = \tau_0$ -hypersurface corresponds to a smooth Cauchy horizon diffeomorphic to \mathbb{S}^3 ruled by closed null curves. In the first case we will call the Cauchy horizon “non-degenerate”, in the second case “degenerate”. This corresponds to the terminology of [32] which can be seen by constructing extensions in “Gaussian null coordinates”. figure 1 depicts a conformal diagram of a singular λ -Taub solution. In that figure, circles correspond to $\tau = \text{const}$ -hypersurfaces, the bold circle represents \mathcal{J}^+ and the dashed circle the Cauchy horizon. We will be particularly interested in the non-degenerate case here. Note that we will often abuse terminology and speak, instead of λ -Taub, often of λ -Taub-NUT.

Singular λ -Taub solutions seem to be counter examples to SCC. Within the Bianchi IX class for $\lambda = 0$, the analogous Taub-NUT spaces [46, 33] for $\lambda = 0$ have been shown to be non-generic in a well-defined sense [40]. For $\lambda > 0$ one believes that the same holds, but no such rigorous result has been found yet. A more general extensively studied symmetry class is Gowdy symmetry which we discuss in the following subsection. In general, further relevant rigorous results concerning SCC for solutions with spatial \mathbb{S}^3 -topology are [32, 21, 31].

2.4. Coordinates and Gowdy spacetimes

Gowdy symmetry [25] is defined by the presence of a smooth effective isometric action of the group $U(1) \times U(1)$ with spacelike orbits. As summarized in [13], if we restrict to smooth orientable connected compact spatial 3-manifolds, the only admitted spatial topologies are \mathbb{T}^3 , $\mathbb{S}^1 \times \mathbb{S}^2$ and \mathbb{S}^3 (and lens spaces which are always included in the following discussion without further comment). Any two of such group actions on one of these topologies are equivalent in the sense of [13].

For the latest state of knowledge in the class of \mathbb{T}^3 -Gowdy spacetimes, we refer to [41, 42] and references therein; we rather focus on the \mathbb{S}^3 -case here. A representation of the action of the Gowdy group on \mathbb{S}^3 is given by

$$\begin{aligned} x_1 &= \cos \frac{\chi}{2} \cos \lambda_1, & x_2 &= \cos \frac{\chi}{2} \sin \lambda_1, \\ x_3 &= \sin \frac{\chi}{2} \cos \lambda_2, & x_4 &= \sin \frac{\chi}{2} \sin \lambda_2, \end{aligned} \quad (5)$$

where we assume the standard embedding of \mathbb{S}^3 into \mathbb{R}^4 . The parameter $\chi \in [0, \pi]$ labels the group orbits while λ_1 and λ_2 , both defined on $\mathbb{R} \bmod 2\pi$, can be considered as the group parameters. The action degenerates exactly when $\chi = 0$ or $\chi = \pi$, i.e. the group orbits become one dimensional. These submanifolds of \mathbb{S}^1 -topology are referred to as symmetry axes in the following. By abusing the terminology slightly, we often also speak of the south pole when we mean the symmetry axis given by $\chi = \pi$; analogously, by north pole we mean the axis given by $\chi = 0$. Equation (5) can also be considered as the defining equation for a coordinate patch on \mathbb{S}^3 ; these coordinates $(\chi, \lambda_1, \lambda_2)$ are called Euler angle parametrization. We will however rather use the coordinates (χ, ρ_1, ρ_2) determined by

$$\lambda_1 = (\rho_1 + \rho_2)/2, \quad \lambda_2 = (\rho_1 - \rho_2)/2.$$

The Euler angle parametrization covers smoothly the dense subset of $\tilde{\mathbb{S}}^3 \subset \mathbb{S}^3$ which is \mathbb{S}^3 minus those points given by $\chi = 0$ or $\chi = \pi$ where the coordinates become singular. Our choice of representation of the frame $\{Y_a\}$ yields the following expressions

$$Y_1 = 2 \sin \rho_1 \partial_\chi + 2 \cos \rho_1 (\cot \chi \partial_{\rho_1} - \csc \chi \partial_{\rho_2}), \quad (6a)$$

$$Y_2 = 2 \cos \rho_1 \partial_\chi - 2 \sin \rho_1 (\cot \chi \partial_{\rho_1} - \csc \chi \partial_{\rho_2}), \quad (6b)$$

$$Y_3 = 2 \partial_{\rho_1}. \quad (6c)$$

Now, on a Gowdy-invariant spacetime with spatial \mathbb{S}^3 -topology let us choose spacetime coordinates $(t, \chi, \lambda_1, \lambda_2)$ such that the $t = \text{const}$ -hypersurfaces are Cauchy surfaces, and such that on a $t = t_0$ -hypersurface Σ_0 the Gowdy orbits are $\chi = \text{const}$ -surfaces parametrized canonically as above by λ_1 and λ_2 . On Σ_0 , a Killing algebra basis is $\{\partial_{\lambda_1}, \partial_{\lambda_2}\}$, but also $\{Y_3, Z_3\}$ where $\{Z_a\}$ are $SU(2)$ -right invariant vector fields defined in the same way as $\{Y_a\}$ before; in particular $Z_3 = 2 \partial_{\rho_2}$. Let us now extend the fields Y_3 and Z_3 from Σ_0 to the spacetime by means of the conditions $[\partial_t, Y_3] = [\partial_t, Z_3] = 0$. Then it is clear directly that $\{Y_3, Z_3\}$ is a basis of the Killing algebra at every instance of time if and only if this is the case for $\{\partial_{\lambda_1}, \partial_{\lambda_2}\}$. It is obvious that the latter does not need to be fulfilled for all foliations; however, it is true in our gauge [7] and also in areal gauge defined below.

The issues of SCC and the BKL-conjecture in the \mathbb{S}^3 -Gowdy class have so far only been solved in the polarized vacuum case with $\lambda = 0$ [29, 12]. In particular, there is a nice characterization of those non-generic Gowdy-invariant data whose MGH is extendible through a Cauchy horizon. For the non-polarized case, both issues are

open. From the results obtained in the \mathbb{T}^3 -case, one expects that spikes are present generically at the singularity, but in particular the behavior at the symmetry axes is not completely understood [45]. The purpose of our investigations is to shed further light on SCC and the issue of spikes for \mathbb{S}^3 -Gowdy perturbations of the λ -Taub-NUT family. Similar numerical investigations in the $\mathbb{S}^1 \times \mathbb{S}^2$ -case have been carried out in [24].

Let us introduce the notion of the orbit area density. This quantity is defined as $\sqrt{\det(g(\partial_{\lambda_a}, \partial_{\lambda_b}))}$ ($a = 1, 2$). In the \mathbb{S}^3 -case one can show that it is proportional to $\sin \chi$ and we will speak of the rescaled orbit area density when this factor has been divided out. For $\lambda = 0$ in vacuum, Chruściel [13] succeeded in showing that an open subset of the MGHD corresponding to generic Gowdy-invariant Cauchy data can be covered by an areal foliation, i.e. a foliation of spacelike hypersurfaces given by the level sets of the rescaled orbit area density, and that the orbits reach zero area either at the boundary of the MGHD or in the interior. In the polarized case, the result is stronger, namely, that the boundary of the MGHD is attained exactly where the orbit area vanishes in the generic case. There are no such results for $\lambda > 0$. In particular, it cannot be expected that solutions which collapse and later re-expand due to the repelling force of the cosmological constant can be covered completely by areal foliations.

Other aspects of Gowdy symmetry and the more general $U(1)$ -symmetry which are needed to develop our numerical method are summarized in [9]. In particular, it is explained there how our formulation of the equations can be reduced to $(1+1)$ dimensions in the Gowdy case in an indirect manner, since it is not possible directly. We should point out that this reduction allows us to restrict to the coordinate locations $\rho_1 = 0$ and an arbitrary (fixed) value of ρ_2 . Hence effectively the unknowns depend only on (t, χ) and our problem reduces to $1+1$ in the Gowdy case. All our computations here take place at $\rho_1 = 0$; the solution at other points can be computed from the formulae in [9] straight forwardly.

2.5. Class of initial data

As initial data on \mathcal{J}^+ for the CFE in Levi-Civita conformal Gauß gauge, we use the data derived for $U(1)$ - and Gowdy symmetry in [7], see also [9]. Here we restrict to Gowdy symmetry. We make no claims about the genericity of these data even in the class of Gowdy data. Under the conventions above, the first part of the data take following form

$$(e_a^b) = \text{diag}(1, 1, a), \quad (7a)$$

$$(\chi_{ab}) = \text{diag}(-1, -1, -1), \quad (7b)$$

$$\Gamma_1^1{}_2 = 0, \quad \Gamma_1^2{}_3 = -1/a, \quad \Gamma_2^1{}_2 = 0, \quad \Gamma_2^1{}_3 = 1/a, \quad (7c)$$

$$\Gamma_2^2{}_3 = 0, \quad \Gamma_3^1{}_2 = 1/a - 2a, \quad \Gamma_3^1{}_3 = 0, \quad \Gamma_3^2{}_4 = 0, \quad (7d)$$

$$(L_{ab}) = \text{diag}\left((5 - 3/a^2)/2, (5 - 3/a^2)/2, (-3 + 5/a^2)/2\right), \quad (7e)$$

$$(B_{ab}) = \text{diag}\left(-4(1 - a^2)/a^3, -4(1 - a^2)/a^3, 8(1 - a^2)/a^3\right). \quad (7f)$$

The induced conformal 3-metric of \mathcal{J}^+ is a Berger sphere with anisotropy parameter $a > 0$ and an adapted orthonormal frame which is expressed by (7a). Now, the only inhomogeneous part of the initial data is given by the components of E_{ab} . In order to construct solutions of the constraint $D^a E_{ab} = 0$ on the background defined by

the expressions above, we expand the components of E_{ab} in terms of spin-weighted spherical harmonics on \mathbb{S}^3 , which under the assumption of $U(1)$ -symmetry are related to spherical harmonics w_{np} on \mathbb{S}^2 . For our definition of the functions w_{np} consult [7]. We restrict to solutions with $n = 0$ and $n = 2$. Then the expressions are

$$(E_{ab}) = \begin{pmatrix} E_0 + \varepsilon w_{20} & 0 & -\sqrt{2} a \varepsilon \operatorname{Re} w_{21} \\ 0 & E_0 + \varepsilon w_{20} & -\sqrt{2} a \varepsilon \operatorname{Im} w_{21} \\ -\sqrt{2} a \varepsilon \operatorname{Re} w_{21} & -\sqrt{2} a \varepsilon \operatorname{Im} w_{21} & -2(E_0 + \varepsilon w_{20}) \end{pmatrix}.$$

With respect to the Euler angle coordinates at $\rho_1 = 0$ we have

$$w_{20} = \cos \chi, \quad w_{21} = \sin \chi / \sqrt{2}.$$

The parameter E_0 is associated with the part of the data given by $n = 0$, while ε parametrizes the inhomogeneous $n = 2$ part.

Note that the solution corresponding to a general choice of parameters in this family is of unpolarized Gowdy type. This has already been claimed in [7]; however, there the argument turned out to be incomplete. In general, we call two initial data sets equivalent if the corresponding MGHDs are isometric. In particular, two initial data sets on \mathcal{J}^+ are equivalent if there is a diffeomorphism from \mathcal{J}^+ to itself such that the pullback of all data fields equals the corresponding fields in the other data set, up to gauge transformations. In our special class of initial data now we find that two initial data sets, one given by ε_1 and the other by $\varepsilon_2 = -\varepsilon_1$, both with the same $a > 0$ and $E_0 \in \mathbb{R}$, are equivalent by means of the diffeomorphism from \mathbb{S}^3 to itself represented by $(x_1, x_2, x_3, x_4) \mapsto (x_3, x_4, x_1, x_2)$. In terms of the Euler coordinates, this diffeomorphism takes the form $(\chi, \rho_1, \rho_2) \mapsto (\pi - \chi, \rho_1, -\rho_2)$. Hence without loss of generality we can assume that $\varepsilon \geq 0$. For $\varepsilon = 0$, the corresponding MGHD of \mathcal{J}^+ is a λ -Taub spacetime whose parameters (D_0, C_0) can be identified with our initial data parameters by

$$a = 1/\sqrt{D_0}, \quad E_0 = C_0 \sqrt{D_0}/2,$$

for $\lambda = 3$. In Levi-Civita conformal Gauß gauge, all τ -level sets are also t -level sets. Note however that our convention is that ∂_τ is future directed while ∂_t is past directed so that \mathcal{J}^+ is given by $t = 0$ and $\tau \rightarrow +\infty$, respectively.

We note that in our formulation of the equations, choice of gauge and with the choice of data above, the following “boundary conditions” for the fields E_{ab} and B_{ab} are implied at each instant of time [9]. Introducing the new fields

$$E_{11}^* := (E_{11} + E_{22})/2, \quad E_{22}^* := (E_{11} - E_{22})/2,$$

and similar for the magnetic part B_{ab} , we find on both symmetry axes at each instant of time

$$E_{12} = E_{13} = E_{22}^* = E_{23} = 0, \quad B_{12} = B_{13} = B_{22}^* = B_{23} = 0, \quad (8)$$

whereas E_{11}^* and B_{11}^* are not restricted. Similar properties are obeyed by all symmetric Gowdy-invariant covariant 2-tensor fields, for instance χ_{ab} . Also, one can derive analogous conditions for some of the connection coefficients which we do not write here. In addition, the constraints of the Bianchi system (3) imply on both axes

$$\partial_\chi E_{11}^* = \partial_\chi E_{22}^* = \partial_\chi B_{11}^* = \partial_\chi B_{22}^* = 0. \quad (9)$$

2.6. Numerical approach

The numerical method which we apply in this paper will not be discussed here, see [9] for that. In summary, it is a pseudospectral single patch approach; as coordinates on \mathbb{S}^3 we decided for the Euler angle parametrization. The relevant singular terms are then determined by the coordinate components of the reference frame $\{Y_a\}$ in (6a)-(6c). We succeeded in regularizing spectrally the formally singular terms in the equations [9].

For our investigations here we made the following special choices which have not yet been fixed in [9]. First, we decided to use no automatic adaption for the spatial resolution. Namely, it turned out to be more convenient to control the spatial resolution manually in order to study convergence of the code at very late times. As the time integrator we decided for the adaptive fifth order “embedded” Runge Kutta scheme [38]. Further, we found that it is necessary to enforce the boundary conditions (8) at each time step in order to keep the code stable at very late times of the evolution; more details about our “partial enforcement” scheme can be found in [9]. Last but not least we mention that we did not use the quad-precision option of the Intel compiler [28]. Except for very small values of ε , see more comments later, double-precision turned out to be sufficient and the constraint growth was more or less under control.

3. Results and their analysis

3.1. Setup and main results

Our strategy to analyze the properties of solutions close to the λ -Taub-NUT family is as follows. For fixed λ -Taub-NUT background spacetimes, i.e. for given values of a and E_0 , we compute and analyze the solutions corresponding to initial data given by several small values of $\varepsilon \geq 0$. In [7] we have speculated that λ -Taub-NUT Cauchy horizons might be stable for small ε in the sense that a smooth Cauchy horizon eventually forms for all $0 \leq \varepsilon < \varepsilon_{crit}$ for some $\varepsilon_{crit} > 0$. The analysis there was done on the basis of a numerical code, namely the $(2+1)$ -code in [9], which was not well adapted to the demands of the problem. Here we report on results obtained with the new $(1+1)$ -code introduced in [9] which allows much more reliable investigations. The main reason is that with the $(1+1)$ -code no spatial resolution is wasted in one of the symmetry directions; recall however that a direct reduction to $(1+1)$ in our formulation is not possible. We still use the same gauge and formulation of the equations as in the $(2+1)$ -code.

Let us choose the parameters a and E_0 such that the λ -Taub-NUT solution corresponding to $\varepsilon = 0$ has a non-degenerate Cauchy horizon, and let t_{TN} be the corresponding critical coordinate time in Levi-Civita conformal Gauß gauge. Our investigations suggest the following results which supersede the previous speculations.

- (i) For each $\varepsilon > 0$, there is a time $0 < t_\varepsilon < t_{TN}$ when the curvature blows up; further $t_\varepsilon \nearrow t_{TN}$ for $\varepsilon \searrow 0$.
- (ii) The mechanisms driving the blow up are “qualitatively independent” of ε (in the sense below); hence blow up takes place always “in the same way” in this family.
- (iii) The standard continuity property holds: the smaller $\varepsilon > 0$, the longer the corresponding solutions stays close to the λ -Taub-NUT solution given by $\varepsilon = 0$.

These results suggest that SCC is true in this class of solutions. Below we give more details on the dynamical processes which seem to give rise to SCC.

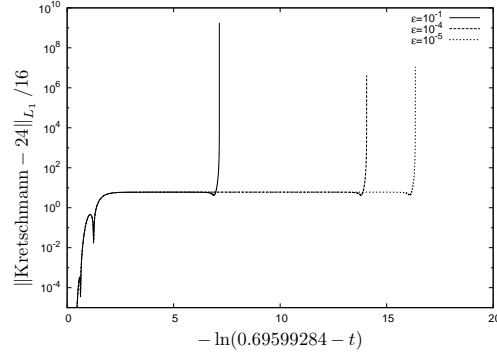


Figure 2. Curvature blow up for various values of ε

In all of our numerical investigations below we choose $a = 0.7$ and $E_0 = 0$, and the reason is the following. Our aim is to study perturbations of spacetimes with a Cauchy horizon, and this is the case for all λ -Taub-NUT solutions with, for instance, $E_0 = 0$, and $a \leq \sqrt{3}/2 \approx 0.866$ (for $\lambda = 3$). We expect that qualitatively the results do not depend strongly on these parameters if the parameters stay in a regime in which the background Cauchy horizon is non-degenerate. This is the case e.g. for all $a < \sqrt{3}/2$ and $E_0 = 0$. The situation might of course be very different when the background is of degenerate type, for instance for $a = \sqrt{3}/2$ and $E_0 = 0$, however, we do not study that case here. For $a = 0.7$, we have $t_{TN} \approx 0.69599284$.

figure 2 shows the numerical plot of a spatial norm[¶] of the physical Kretschmann scalar versus time for various values of ε . In that plot, we have normalized the time axis such that the critical time t_{TN} of the unperturbed solution is at roughly 20. The smallest value of ε in our numerical series was 10^{-5} , see comments on this below. Note that more details on the numerical properties of the solutions, at least in the case $\varepsilon = 10^{-1}$, are available in [9].

3.2. Heuristic discussions of dynamical effects

3.2.1. Preparations Now we discuss the numerical results in a more detailed way and complement them with heuristic arguments in order to give some explanations and extrapolations of our results. A rigorous discussion would be clearly preferable, however, is believed to be extremely difficult since many terms with their individual sign structures seem to be significant for the dynamics. One advantage of a numerical approach is that it can be expected to provide information in particular on intermediate evolution times. This might shed light on for instance the question which dynamical processes are responsible to implement SCC. The idea for the following heuristic discussion is to consider the linearization of the evolution equation for small $\varepsilon > 0$ around the λ -Taub-NUT solution given by $\varepsilon = 0$. One can believe that this yields a good approximation for small ε and small t . Unexpectedly, we find below that a discussion exclusively based on the linearized equations already fails at early times, i.e. in a small past neighborhood of \mathcal{J}^+ . However, by taking into account some nonlinear effects supplementing the linearized equations, we are able to obtain some insights. It should be noted that we are only interested in qualitative arguments now

[¶] This norm is the L^1 -norm on \mathbb{S}^3 , however, as mentioned in [9], the volume element of the Euler angle coordinates is left out in the integral.

and that none of the simplifying assumptions or approximations considered in the following are used for the numerical calculations. We point out again, that our time coordinate which we always refer to runs backward in time, i.e. when we speak, e.g. of the early phase of the evolution we mean the dynamics close to \mathcal{J}^+ , hence very far in the future from the physical point of view. After these discussions, we also elaborate on the limitations of the current results and hence what remains to be done in future work.

In order to proceed with the linearization we write for the unknowns

$$e_a^b = \dot{e}_a^b + \varepsilon \hat{e}_a^b, \quad \chi_{ab} = \dot{\chi}_{ab} + \varepsilon \hat{\chi}_{ab}, \quad \Gamma_a^b{}_c = \dot{\Gamma}_a^b{}_c + \varepsilon \hat{\Gamma}_a^b{}_c, \quad \dots,$$

where higher order terms in ε , which are in principle present for some of these unknowns, have already been neglected. Below we express some of the background λ -Taub-NUT components, marked by \circ , by means of functions $a_1(t)$ and $a_3(t)$ and their time derivatives such that

$$\begin{aligned} (\dot{e}_a^b)(t) &= \text{diag}(a_1(t), a_1(t), a_3(t)), \\ (\dot{\chi}_{ab})(t) &= \text{diag}(-a_1'(t)/a_1(t), -a_1'(t)/a_1(t), -a_3'(t)/a_3(t)), \\ \dot{\Gamma}_3^1{}_2(t) &= a_1(t)^2/a_3(t) - 2a_3(t), \quad \dot{\Gamma}_1^2{}_3 = -\dot{\Gamma}_2^1{}_3 = -a_1(t)^2/a_3(t); \end{aligned}$$

all other connection coefficients of the background vanish. Here, a prime denotes the derivative with respect to the time t of the λ -Taub-NUT solution given by $\varepsilon = 0$. The function $a_3(t)$ equals the initial data parameter a before at $t = 0$, further $a_1(0) = 1$. The explicit form of the functions $a_1(t)$ and $a_3(t)$ can be derived from the relations given in section 2.3; however, in order to evaluate the transformation from Brill's time coordinate τ to our time coordinate t one has to compute an integral which in general cannot be represented in closed form. In any case, in order to keep the expressions below as short as possible, the other three distinct non-vanishing functions of the background $\dot{L}_{11} = \dot{L}_{22}$, \dot{E}_{11}^* and \dot{B}_{11}^* are not written out in terms of $a_1(t)$, $a_3(t)$ and their derivatives in the following.

Note that for the full evolution equations with our choice of gauge and frame, the 1-2- and 2-3-components of all covariant 2-tensor fields in the set of unknowns are identically zero for all times at $\rho_1 = 0$. Also some of the components of the connection coefficients vanish there. Hence, we do not need to consider their evolution equations. Further we restrict our attention now to the evolution equations of the electric and magnetic parts of the rescaled Weyl tensor (the Bianchi system) since those describe the evolution of curvature. Only where necessary, also the other equations are taken into account. With $F(\chi) := -2 \cot \chi$, the linearized evolution equations take the following form

$$\begin{aligned} \partial_t \hat{E}_{22}^* &= \underbrace{-\frac{1}{2}a_1(2\partial_\chi + F(\chi))\hat{B}_{13}}_{\text{Term IV}} - \underbrace{\frac{a_1^2 \hat{B}_{22}^*}{a_3}}_{\text{Term II}} + \underbrace{\left(\frac{a_1'}{a_1} + \frac{2a_3'}{a_3}\right)\hat{E}_{22}^*}_{\text{Term I}} \\ &\quad + \underbrace{\frac{3}{2}\hat{B}_{11}^* \left(\hat{\Gamma}_1^2{}_3 + \hat{\Gamma}_2^1{}_3\right) + \frac{3}{2}\hat{E}_{11}^* \left(\hat{\chi}_{11} - \hat{\chi}_{22}\right)}_{\text{Term V}}, \end{aligned} \tag{10a}$$

$$\begin{aligned} \partial_t \hat{B}_{22}^* = & \underbrace{\frac{1}{2} a_1 (2\partial_\chi + F(\chi)) \hat{E}_{13}}_{\text{Term IV}} + \underbrace{\frac{a_1^2 \hat{E}_{22}^*}{a_3}}_{\text{Term II}} + \underbrace{\left(\frac{a'_1}{a_1} + \frac{2a'_3}{a_3} \right) \hat{B}_{22}^*}_{\text{Term I}} \\ & - \underbrace{\frac{3}{2} \hat{E}_{11}^* \left(\hat{\Gamma}_{1\ 3}^2 + \hat{\Gamma}_{2\ 3}^1 \right) + \frac{3}{2} \hat{B}_{11}^* \left(\hat{\chi}_{11} - \hat{\chi}_{22} \right)}_{\text{Term V}}, \end{aligned} \quad (10b)$$

$$\begin{aligned} \partial_t \hat{E}_{13} = & \underbrace{3a_1 \partial_\chi \hat{B}_{11}^*}_{\text{Term III}} + \underbrace{a_1 (\partial_\chi - F(\chi)) \hat{B}_{22}^*}_{\text{Term IV}} \\ & + \underbrace{\frac{2a_1^2 \hat{B}_{13}}{a_3}}_{\text{Term II}} + \underbrace{\left(\frac{5a'_1}{2a_1} + \frac{a'_3}{2a_3} \right) \hat{E}_{13}}_{\text{Term I}} - \underbrace{\frac{3}{2} \hat{B}_{11}^* \hat{\Gamma}_{3\ 3}^2 - \frac{3}{2} \hat{E}_{11}^* \hat{\chi}_{13}}_{\text{Term V}}, \end{aligned} \quad (11a)$$

$$\begin{aligned} \partial_t \hat{B}_{13} = & \underbrace{-3a_1 \partial_\chi \hat{E}_{11}^*}_{\text{Term III}} - \underbrace{a_1 (\partial_\chi - F(\chi)) \hat{E}_{22}^*}_{\text{Term IV}} \\ & - \underbrace{\frac{2a_1^2 \hat{E}_{13}}{a_3}}_{\text{Term II}} + \underbrace{\left(\frac{5a'_1}{2a_1} + \frac{a'_3}{2a_3} \right) \hat{B}_{13}}_{\text{Term I}} + \underbrace{\frac{3}{2} \hat{E}_{11}^* \hat{\Gamma}_{3\ 3}^2 - \frac{3}{2} \hat{B}_{11}^* \hat{\chi}_{13}}_{\text{Term V}}, \end{aligned} \quad (11b)$$

$$\begin{aligned} \partial_t \hat{E}_{11}^* = & \underbrace{-\frac{1}{2} a_1 (2\partial_\chi - F(\chi)) \hat{B}_{13}}_{\text{Term III}} + \underbrace{\frac{3a_1^2 \hat{B}_{11}^*}{a_3}}_{\text{Term II}} + \underbrace{\frac{3a'_1 \hat{E}_{11}^*}{a_1}}_{\text{Term I}} \\ & - \underbrace{\frac{3}{2} \hat{B}_{11}^* \left(\hat{\Gamma}_{1\ 3}^2 - \hat{\Gamma}_{2\ 3}^1 \right) - \frac{3}{2} \hat{E}_{11}^* \left(\hat{\chi}_{11} + \hat{\chi}_{22} \right)}_{\text{Term V}}, \end{aligned} \quad (12a)$$

$$\begin{aligned} \partial_t \hat{B}_{11}^* = & \underbrace{\frac{1}{2} a_1 (2\partial_\chi - F(\chi)) \hat{E}_{13}}_{\text{Term III}} - \underbrace{\frac{3a_1^2 \hat{E}_{11}^*}{a_3}}_{\text{Term II}} + \underbrace{\frac{3a'_1 \hat{B}_{11}^*}{a_1}}_{\text{Term I}} \\ & + \underbrace{\frac{3}{2} \hat{E}_{11}^* \left(\hat{\Gamma}_{1\ 3}^2 - \hat{\Gamma}_{2\ 3}^1 \right) - \frac{3}{2} \hat{B}_{11}^* \left(\hat{\chi}_{11} + \hat{\chi}_{22} \right)}_{\text{Term V}}. \end{aligned} \quad (12b)$$

In order to avoid confusions we point out that studying solutions of these equations, which originate in a linearization around a λ -Taub-NUT spacetime, is fundamentally different from considering the spin-2 system, i.e. the Bianchi system, on the same λ -Taub-NUT background. Both lead to a similar, but distinct set of equations. In the latter case, which is not of interest here, certain consistency conditions [37] must be satisfied, otherwise no solutions need to exist at all.

3.2.2. Dynamical effects at early times

Oscillatory phase In this earliest phase in the past of \mathcal{J}^+ , the “evolution makes a decision on the signs of the quantities” by performing a couple of oscillations before going over to a more or less monotonic behavior. Consider the linearized evolution equations (10a) and (10b) first. We know from our choice of initial data that both \hat{E}_{22}^* and \hat{B}_{22}^* are zero at $t = 0$. If this is true at some other time, the equations imply that also their time derivatives are zero, if additionally $\hat{\chi}_{11} = \hat{\chi}_{22}$,

$\hat{\Gamma}_1^2{}_3 = -\hat{\Gamma}_2^1{}_3$ (term V) and \hat{B}_{13} and \hat{E}_{13} are proportional to $\sin \chi$ (term IV); note here that $(2\partial_\chi + F(\chi)) \sin \chi = 0$. This is the case initially. Checking the linearized evolution equations for $\hat{\chi}_{11} - \hat{\chi}_{22}$ and $\hat{\Gamma}_1^2{}_3 + \hat{\Gamma}_2^1{}_3$, which are not printed here, one finds that also their time derivatives are zero in that case. Further, due to the linearity of the equations and due to the required behavior at the boundaries, \hat{E}_{13} and \hat{B}_{13} must be proportional to $\sin \chi$ for all times. In summary, the linearized evolution equations imply that for these initial data, \hat{E}_{22}^* and \hat{B}_{22}^* are zero identically for all times. Nevertheless, we find numerically that \hat{E}_{22}^* and \hat{B}_{22}^* are non-zero for $t > 0$. In fact, they grow so strongly that they become dominant after a short time. Hence a discussion which is exclusively based on the linearized equations with these initial data would miss this important character of the solution. This fact is related to the results in [4] which however restricts to $\lambda = 0$. A simple nonlinear mechanism driving \hat{E}_{22}^* and \hat{B}_{22}^* away from zero is the following. If due to nonlinear dynamics there is a small higher order component, say,

$$\hat{B}_{13}(t, \chi) = \hat{B}_{13}^{(0)}(t) \sin \chi + \hat{B}_{13}^{(1)}(t) \sin 2\chi \quad (13)$$

with $\hat{B}_{13}^{(1)} \ll \hat{B}_{13}^{(0)}$, then term IV in (10a) yields

$$(2\partial_\chi + F(\chi))\hat{B}_{13} = -4\hat{B}_{13}^{(1)} \sin^2 \chi.$$

Indeed we find numerically that the early dynamics can be described very well as

$$\hat{E}_{22}^*(t, \chi) = \hat{E}_{22}^{*(0)}(t) \sin^2 \chi; \quad (14)$$

the same holds for the magnetic component. Another conceivable lowest order contribution to \hat{E}_{13} and \hat{B}_{13} is one which is proportional to $\cos \chi$, but then according to the boundary conditions (8), there must also be a term proportional to $\cos 3\chi$ which is of higher order and can be neglected so far. Another possibility consistent with the boundary conditions is of the form $1 - \cos 2\chi$. However then it turns out that term IV in (10a) and (10b) violates (9), i.e. the boundary conditions implied by the Bianchi constraints. Hence (13) is the lowest order explanation for (14). In any case, as soon as \hat{E}_{22}^* and \hat{B}_{22}^* have been driven away from zero, the linearized equations govern their evolution, in particular terms I and II, see below. term IV does not become significant before $\hat{B}_{13}^{(1)}$ in (13) has become large enough in comparison to $\hat{B}_{13}^{(0)}$; the same for the electric component. At early times, we also find that terms V can be neglected. One explanation is the following. When t is small, the only significant sources in the linearized evolution equations for the quantities $\hat{\chi}_{11} - \hat{\chi}_{22}$ and $\hat{\Gamma}_1^2{}_3 + \hat{\Gamma}_2^1{}_3$ are the quantities \hat{E}_{22}^* and \hat{B}_{22}^* which are however very small. Hence these quantities are even smaller. Now, since \hat{E}_{11}^* and \hat{B}_{11}^* are not larger than order unity for all times, this implies that term V can be neglected for small t . What is the effect of terms I and II? At early times a_1 and a_3 differ only slightly, further $a'_b/a_b \sim 1$ ($b = 1, 3$) due to the choice of initial data, and thus term II can be of the same order of magnitude as term I. Indeed, the sign structure of these terms implies oscillations of the amplitudes $\hat{E}_{22}^{*(0)}(t)$ and $\hat{B}_{22}^{*(0)}(t)$ in time. Now, both of a_1 and a_3 are monotonically increasing, but a_3 eventually stronger than a_1 . These oscillations stop when a_3 becomes so big in comparison to a_1 that term II cannot have an significant effect anymore; note that in particular a'_3/a_3 is strongly monotonically increasing as being proportional to $\hat{\chi}_{33}$. The oscillations die out relative early, and in our notation above $\hat{E}_{22}^{*(0)}(t) < 0$ and $\hat{B}_{22}^{*(0)}(t) > 0$ from then on. Then, term I leads to strong growth of the absolute values of the amplitudes. We find numerically, that $|\hat{E}_{22}^{*(0)}(t)| > |\hat{B}_{22}^{*(0)}(t)|$ for all following

early times so that there is a net effect for the Kretschmann scalar (4). Later in the evolution, this growth becomes dominant and eventually seems to lead to blow up of the Kretschmann scalar. In figure 3, we see a plot of the spatial distribution of these components at a time for which our discussion so far is still valid. However, first signs of further nonlinear effects become significant which we will discuss later.

Next consider the linearized evolution equations (11a) and (11b) of \hat{E}_{13} and \hat{B}_{13} . The early evolution takes place in a similar way as before. The main difference is now however that the initial data of \hat{E}_{13} is non-vanishing and hence the linear effects described by these equations dominate the nonlinear ones at the beginning. In the same way as above, terms I and II are dominant with a correction in the oscillatory structure by the additional term III. Again, oscillations stop when term II becomes insignificant in comparison to term I. The influence of term V is different than before. Namely, by checking the signs and magnitudes of $\hat{\Gamma}_3^2{}_3$ and $\hat{\chi}_{13}$ numerically, term V can be seen to become significant a bit later in the evolution. Then it decelerates the growth of \hat{E}_{13} and \hat{B}_{13} , and so they do not blow up as quickly as \hat{E}_{22}^* and \hat{B}_{22}^* above. The significance of term IV becomes obvious later. For the whole early time, \hat{E}_{13} and \hat{B}_{13} can be described very well as proportional to $\sin \chi$, and we find numerically that their amplitudes are negative from the time on at which oscillations stop; consider again figure 3. In particular, the plot shows nicely the different rates of growth for the components discussed so far; compare also to figure 4.

The discussion of \hat{E}_{11}^* and \hat{B}_{11}^* and their linearized evolution equations (12a) and (12b) is very similar. Again term I and II are dominant at early times and lead to oscillations in time with corrections by term III. Eventually, after these have stopped, term V decelerates the growth similarly as in the 1-3-case so that they grow much less than in particular \hat{E}_{22}^* and \hat{B}_{22}^* . Both \hat{E}_{11}^* and \hat{B}_{11}^* can be described well as proportional to $\cos \chi$ with eventually positive amplitudes.

For understanding the limit $\varepsilon \rightarrow 0$, one should be worried whether the relevant terms in the equations are of different relative magnitude for different values of ε . If yes, there would be a dependence of the character of the early oscillations on ε , and this could lead to a different sign structure of the solution eventually. Most likely this would mean that the late time behavior, i.e. close to the critical time, depends strongly on ε . However, the structure of the linearized evolution equation and the initial data are such, that the amplitudes of the dominant terms at early times have a consistent scaling with ε . Hence the early oscillations are, apart from this scaling, independent of ε . In detail, the dependence of the initial data on ε suggests

$$\hat{E}_{11}^*, \hat{B}_{11}^*, \hat{E}_{13}, \hat{B}_{13} \sim \varepsilon, \quad (15a)$$

which is compatible with the equations. Further it is reasonable to expect

$$\hat{E}_{22}^*, \hat{B}_{22}^* \sim \varepsilon^2. \quad (15b)$$

Indeed, one can check numerically that this scaling holds true for early times, but we will not show this here. As it can be expected, the behavior at later times cannot be described in this simple way anymore.

Intermediate nonlinear phase We proceed with the discussion of that phase of the evolution in which nonlinear effects take over. In that phase, the evolution forms the spatial shapes of the unknowns, and leading order effects are the following. As we have said before, we find (14) for early times induced by the higher order component in (13); similarly for the magnetic component. From the sign structure of \hat{E}_{22}^* and \hat{B}_{22}^* we can

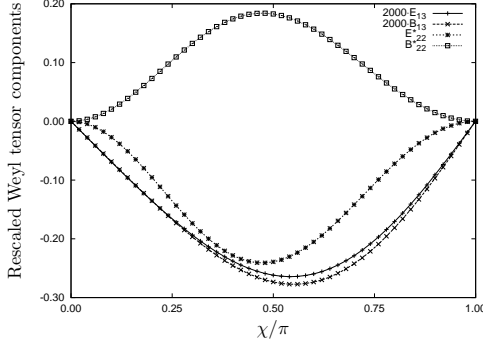


Figure 3. Spatial dependence at $t = 0.69598373$ for $\varepsilon = 10^{-4}$

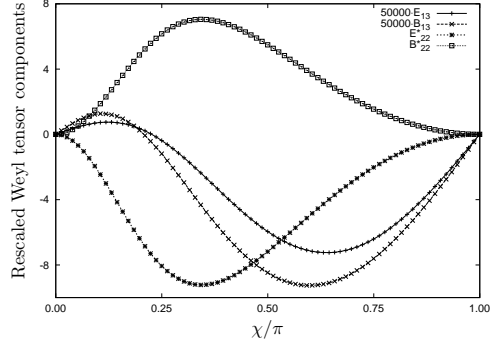


Figure 4. Spatial dependence at $t = 0.69599118$ for $\varepsilon = 10^{-4}$

read off that the sign of this higher order component must be such that the spatial extrema of \hat{E}_{13} and \hat{B}_{13} slowly move to the south pole. Further we find that term IV in (11a) and (11b) is then also proportional to $\sin 2\chi$ with the “right” signs, hence this effect is amplified. In fact this is what we observe numerically, see figure 3. Certainly, such nonlinear interactions are also able to produce a component proportional to $\sin 3\chi$ or $(\cos \chi - \cos 3\chi)$, recall the boundary conditions (8), for \hat{E}_{13} and \hat{B}_{13} . For the latter contribution, term IV in (10a) and (10b) yields a violation of (9), hence must not be present. Consider $\sin 3\chi$. With this, term IV in (10a) and (10b) obtains a component proportional to $\cos \chi \sin^2 \chi$. The effect is that also the extrema of \hat{E}_{22}^* and \hat{B}_{22}^* start to move slowly, however, with this simple description we are not able to deduce the signs of that term and hence the direction of the move. Numerically we see that these extrema move toward the north pole in figure 3 and 4. Now, considering again term IV in (11a) and (11b) with this new component proportional to $\cos \chi \sin^2 \chi$, the quantities \hat{E}_{13} and \hat{B}_{13} obtain an additional contribution of the form $\sin 3\chi$, however, with an amplitude opposite to the previous one; thus the nonlinear interactions must dominate the linear ones here to keep this process alive. We find numerically that the signs eventually become such that the quantities \hat{E}_{13} and \hat{B}_{13} grow positively close to the north pole, while the move of the extrema to the south pole is decelerated. All this is visible in figure 4. Indeed we find eventually that the positive growth of \hat{E}_{13} and \hat{B}_{13} at the north pole becomes much stronger than the dynamics at the south pole.

When comparing different values of ε , one finds that the smaller $\varepsilon > 0$, the later, but eventually the more rapid, all these nonlinear effects take place. One may certainly wonder what is special about, say, the north pole in these spacetimes. This issue becomes clear when one recalls that going from ε to $-\varepsilon$ is equivalent to the interchange of the north and south pole.

3.2.3. Universality and the late time behavior The longer the evolution proceeds, the higher is the order of the significant nonlinear effects. We make no effort here to describe all those. Nevertheless, we find numerically that the qualitative picture described before does not change anymore for late times. Some of the quantities tend to blow up and there is an even stronger concentration of curvature close to $\chi = 0$. Further, the computations suggest that qualitatively the same picture is true for all

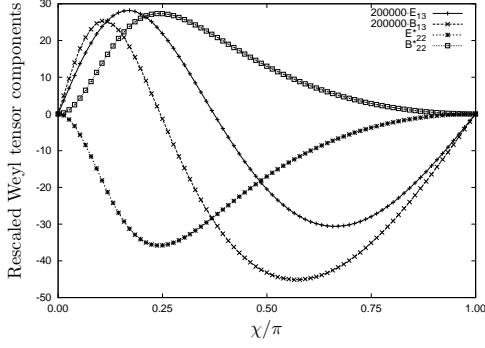


Figure 5. Spatial dependence at $t = 0.69599176$ for $\varepsilon = 10^{-4}$

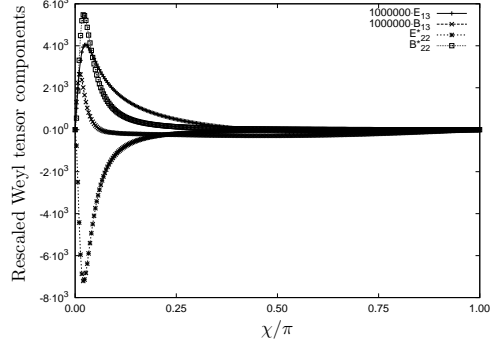


Figure 6. Spatial dependence at $t = 0.69599206$ for $\varepsilon = 10^{-4}$

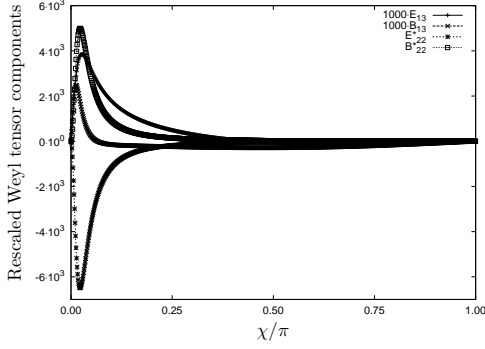


Figure 7. Spatial dependence at $t = 0.69520300$ for $\varepsilon = 10^{-1}$

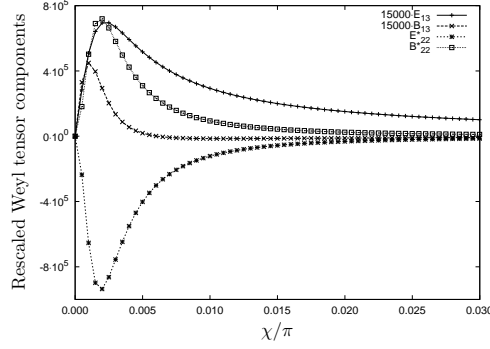


Figure 8. Spatial dependence at $t = 0.69520492$ for $\varepsilon = 10^{-1}$

small values of ε . Certainly, nonlinear effects become significant at a later time the smaller ε is. In particular the magnitude of E_{22}^* and B_{22}^* is smaller in relation to the other components at early times according to the scaling given by (15a) and (15b). But from some time on, and then on a shorter time scale, these overtake and a “universal” qualitative picture is obtained. All this is demonstrated in the numerical plots in figure 5 to 8. As already mentioned, we see particularly strong blow up of E_{22}^* and B_{22}^* . Indeed, this seems to yields the main contribution to the Kretschmann scalar at late times. According to the plots above, E_{13} and B_{13} also grow at the north pole and maybe even blow up eventually. However, this growth seems to be slower. Why does the blow up of curvature seem to be confined to a small region around the north pole? We can give an explanation for this below, and this is most likely caused by our choice of foliation.

However, what happens exactly on the north pole? The only curvature components which do not vanish there according to (8) are E_{11}^* and B_{11}^* which we have said only little about so far. It seems that, as long as we have evolved numerically so far, those stay bounded and the dynamics is very slow. According to their evolution equations, their behavior at $\chi = 0$ depends strongly on the behavior of the χ -derivatives of E_{13} and B_{13} there. The numerical results suggest that those are positive and grow, but relatively slowly. In fact, it seems that their growth is even

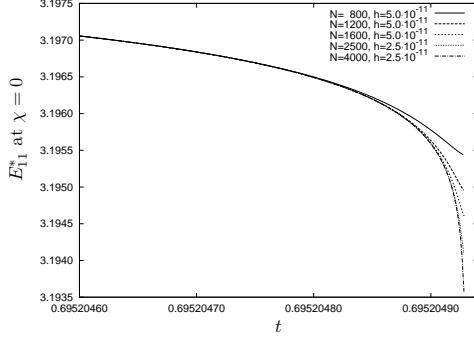


Figure 9. E_{11}^* at $\chi = 0$ for late times

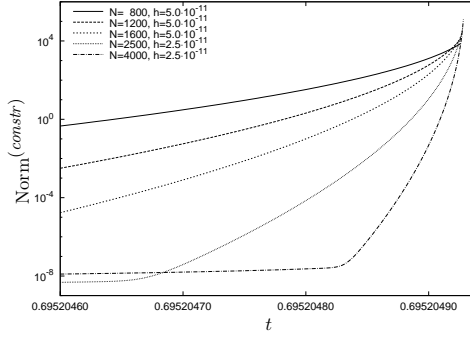


Figure 10. $\text{Norm}^{(constr)}$ for late times

slower in comparison to the growth of E_{22}^* and B_{22}^* the smaller ε is, see figure 5 to 8. In total, it must be said that it is so far an outstanding question if the curvature at $\chi = 0$ stays bounded, in particular for small values of ε . In order to demonstrate how difficult these investigations are with the current numerical setup, figure 9 shows the behavior of E_{11}^* at $\chi = 0$ for times shortly before the numerical solutions blow up for various final numerical resolutions. Here N is the final number of spatial grid points in the χ -direction and h is the final value of the size of the time step, i.e. equals h_{min} as given in [9]. In addition, figure 10 shows the behavior of the constraint violations $\text{Norm}^{(constr)}$ defined in [9]. This plot suggests that the numerical solution converges and that the constraint error can be kept under control for sufficiently high, in particular spatial resolutions at least temporarily. Nevertheless, since on the one hand the demand for resolution at those late times becomes so high, but on the other hand the dynamics of E_{11}^* (also B_{11}^*) at $\chi = 0$ seems to be so slow, we cannot answer the question about the behavior of curvature on the north pole yet. This means that we are also not able yet to exclude the possibility that a strong blow up of E_{11}^* and B_{11}^* at very late times induces a drastic change of the whole asymptotic dynamics. In any case, ideas how to optimize the numerical late time behavior and the setup of our approach are discussed below.

3.3. Further comments on the solutions

3.3.1. Area of the group orbits In section 2.4 we have introduced the notion of the rescaled orbit area for the \mathbb{S}^3 -Gowdy class and have stated that one can believe that a relevant subset of the MGHDs can be covered by areal foliations. In the \mathbb{T}^3 -Gowdy case without cosmological constant the singularity is attained generically exactly where the group orbit area density vanishes. If we are willing to assume that this is true also for our \mathbb{S}^3 -Gowdy solutions with $\lambda > 0$, then we can get a feeling on how “close” the numerical evolutions have eventually approached the “singularity” at the end of the numerical runs by looking at the rescaled orbit area density. Certainly, our foliation is not of areal type, hence this quantity is not constant on our $t = \text{const}$ slices, see figure 11 for a typical late time profile. According to this interpretation, we see that our foliation has approached the singularity further at the north pole than at the south pole which explains why curvature blows up much more strongly there. In fact, figure 12 implies that this discrepancy between the poles, where the

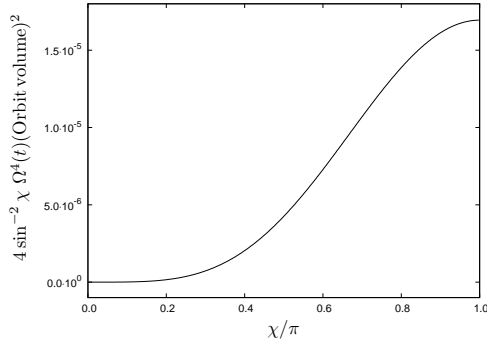


Figure 11. Rescaled orbit area at $t = 0.69520493$ for $\varepsilon = 10^{-1}$

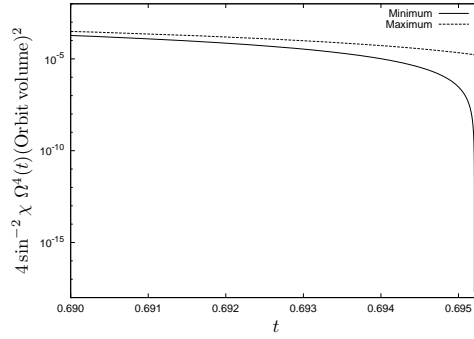


Figure 12. Extremal values of rescaled orbit area for $\varepsilon = 10^{-1}$ on $t = \text{const}$ -slices

maximum and minimum respectively of this rescaled quantity are always attained in our case, becomes larger the further the evolution proceeds. Thus the singularity is approached “inhomogeneously” in this sense in our gauge. We just note that this is not surprising since many gauges which have been used in the literature so far have such a property. Hence one can expect that only special gauges are suitable for our kinds of investigations, and it will be a matter of future research to experiment with such other foliations, see below. Concerning the question of SCC our gauge is thus not appropriate enough. For other open questions, however, as that about the appearance of Gowdy spikes, our computations have the potential to yield new insights.

3.3.2. Gowdy spikes From the results obtained in the \mathbb{T}^3 -Gowdy case, one can expect spikes in the sense of section 2.4 to form under certain conditions at isolated points away from the axes. The previous discussion about the gauge however suggests that we cannot conclude that the local curvature blow up close to the north pole is such a spike. Rather, it can be caused by the “inhomogeneous” approach to the singularity. It is nevertheless possible that spikes show up later in the evolution even in our gauge, but most likely they would be difficult to distinguish from our gauge effects. However, from our numerical data obtained in Levi-Civita conformal Gauß gauge we can – in principle – compute the geometrical quantities with respect to an areal foliation until very “close to the singularity” in a small spatial neighborhood of the north pole. With this it would be feasible to study the possible appearance of spikes there. However, this has not been done yet. In areal gauge, one often introduces a time coordinate τ such that the rescaled orbit area is proportional to $e^{-\tau}$, at least for late times in the \mathbb{S}^3 -case. Hence, a local reconstruction of the areal foliation from the current numerical data would reach Gowdy times of the order $\tau \approx 20$, which is in fact quite impressive. Certainly, it is possible that our family of solutions given by low ε corresponds to “low-velocity” solutions. The concept of the asymptotic velocity is not defined here, see [29, 45] for the \mathbb{S}^3 -case. In fact the relation of this asymptotic quantity at the singularity and our definition of ε as a data parameter on \mathcal{J}^+ is not easy to see. It sounds reasonable that the larger ε is, the higher the asymptotic value of the velocity becomes. Now, in the \mathbb{T}^3 -Gowdy case in vacuum with $\lambda = 0$, one finds that spikes occur only if the asymptotic velocity exceeds a certain value. So we would expect spikes to form in our class of spacetimes away from the axes only for large ε . It is

an unexpected outcome of our numerical experiments that it seems easier to compute solutions for larger ε than for small values, see below. Hence there is hope that spikes can be studied with the current numerical setup. This is planned as a future research topic, but in this paper we are rather concerned with the limit $\varepsilon \rightarrow 0$. Nevertheless, we would like to note that our numerical method can be expected to be able to resolve Gowdy spikes in principle because of our experience with numerical investigation of \mathbb{T}^3 -Gowdy solutions in [7]. The question of the behavior of the solutions on the axes is particularly interesting since, as discussed in [45], although one can expect some discontinuous behavior at the axes in a particular family of parametrizations of the metric, it is not clear whether generic \mathbb{S}^3 -Gowdy solutions have a true spike there. Thus it is remarkable that our numerical results suggest that even at those relatively late Gowdy times, the curvature has not blown up on the axes yet. However, this might of course also be a consequence of the special choice of initial data.

3.4. Limitations and prospects for future work

Our approach of studying the properties of this class of solutions has several limitations so far, some of which were already mentioned above. Some of these limitations are caused by our non-rigorous combination of numerical and heuristic analyzes, and are of principle nature. Others, however, can be avoided more easily and are currently work in progress. In fact we believe that the numerical method has not been pushed to its limits yet.

In our investigations, we are not yet able to conclude finally on the question of SCC in this class of spacetimes, although the numerical results suggest so far consistently that SCC holds in the sense of section 3.1. Nevertheless, we cannot yet deduce the very late time behavior of curvature at the north pole, mainly, but not exclusively, due to numerical problems. Also away from the north pole, we are facing the problem that the foliation does not proceed toward the “singularity” fast enough as was discussed above. Concerning this gauge issue, we would hence like to try various other gauge conditions in future work, for instance areal gauge, which might however be problematic for $\lambda > 0$ in general, but possibly not here. Within the class of general conformal Gauß gauges there is also freedom left which we have not exploited yet. Nevertheless, it is expected that the description of the transport of spatial symmetries is not trivial in general in this gauge. We would like to note that there is also gauge freedom left within the Levi-Civita conformal Gauß gauge, namely to perform an arbitrary conformal transformation of the initial 3-metric and correspondingly of the other data components. It has not been investigated yet if it would be possible to optimize the foliation in this simple way. Other promising gauges are those of harmonic type and constant mean curvature foliations since there is some experience with these in the numerical relativity community. However, for their use with the conformal field equations, it must be investigated first if and how those gauges can be put into the required form.

Concerning the numerical method, there are currently a number of obstacles for driving the numerical solutions “further to the singularity”. Some of those are straight forward to solve, others are not. The runs presented here each took a few hours on single processor machines. It is of course no principle problem to let the runs continue for a few days etc. But at the moment, we have a problem with disk space since our data output routines are not yet optimized; clearly, this problem is straight forward to fix. What are the main reasons that it is numerically demanding to continue the runs?

At the north pole, the solutions develop large gradients, hence much spatial resolution is needed there. So far in our code, resolution cannot be increased locally, and thus increasing the spatial resolution to cope with the demands at the north pole always goes hand in hand with a waste of grid points around the south pole where relatively little happens. Up to now, we have investigated only little on spatial coordinate transformations which would put more spatial points close to the left axis and less to the right axis without a direct change of the numerical infrastructure. In any case, this trick will be studied further in the future. It should be noted that our code is not yet optimized technically for high spatial resolutions in general; in particular we still do not use the Fast Fourier Transform (FFT) [15] yet but only partial summation [10]. Also it may be true that there are more optimal time integrator schemes than the adaptive Runge Kutta schemes of our choice, comments on this can be found in [10]. Further, it might make sense to think about parallelization of the code; this should be straight forward with some publically available FFT libraries as for instance [23]. It is certainly a justified question if a pseudospectral method like ours is suitable at all for this class of problems. Namely, although these methods are highly accurate for lower resolutions they might be too slow for high resolutions. Thus it makes sense to also investigate into other methods, for instance finite differencing methods, maybe even with multipatch or mesh refinement. For instance the similar numerical investigations of Gowdy spacetimes with spatial $\mathbb{S}^1 \times \mathbb{S}^2$ -topology in [24] were done with finite differencing. Another non-related numerical issue shows up for small values of ε at late times. Then, the numerical noise caused by round-off errors can become significant. Indeed, this was the main reason why we did not decrease ε further than 10^{-5} . Maybe, the only solution to this problem is to switch to quad-precision which is possible for Intel compilers and Intel processors, but then the code runs much slower. Further comments on our numerical infrastructure can be found in [9].

A further aspect one should keep in mind is the question about the optimal formulation of Einstein's field equations for our purposes. It is justified to ask if it is necessary to use the conformal field equations for our applications at all. There are two motivations why we decided for these equations. First, prescribing data on \mathcal{J}^+ is simpler than in the case of Cauchy surfaces of the physical spacetime. Second, we wish to study FAdS spacetimes since those are motivated by current cosmological observations and, which is maybe more important here, the MGHD of any data on \mathcal{J}^+ is geodesically complete to the future by construction. So SCC is obeyed at least to the future. In contrast, prescribing data on a Cauchy surface of the physical spacetime yields no a priori knowledge in general whether the corresponding solution is future geodesically complete. Of course, one might want to restrict to the question of SCC in the past direction as a first step. Then, the conformal field equations can be avoided. It is possibly an advantage to rely on the experience of the numerical relativity community which is available for certain formulations of EFE but not so much for the conformal field equations. For instance there exist methods to damp constraint violations etc. Indeed, we have performed successful numerical tests with a well-adapted system other than the CFE in the \mathbb{T}^3 -Gowdy case in [7] and would like to work out a similar system for the \mathbb{S}^3 -case.

4. Summary

In this work, we have presented investigations of the evolution properties of a special class of spacetimes given by certain perturbations of the λ -Taub-NUT solutions. By

means of a combination of numerical and heuristic analyzes, we were able to draw a qualitative picture of the late time behavior of the solutions. The results suggest that SCC holds in this family and we are able to give more details on the dynamical processes which seem to give rise to SCC. However, we are not yet able to make final conclusions. Nevertheless, we identify some of the problems and limitations of our current approach and give prospects for future work. It is surprising that the issue of strong cosmic censorship and of the BKL-conjecture is still open even in this relatively simple class of \mathbb{S}^3 -Gowdy spacetimes. Certainly the family of spacetimes considered here is very special, and it is unclear what information we yield both about the general SCC conjecture and about SCC in the class of general \mathbb{S}^3 -Gowdy spacetimes. We believe however that the results presented here are promising steps in order to derive a consistent picture on these questions in the near future.

Acknowledgments

This work was supported in part by the Göran Gustaffson foundation. We would like to thank in particular Helmut Friedrich, David Garfinkle, Alan Rendall and Hans Ringström for useful discussions, advices and comments.

- [1] M.T. Anderson. Existence and stability of even dimensional asymptotically de Sitter spaces. *Annales Henri Poincare*, 6:801–820, 2005, gr-qc/0408072.
- [2] L. Andersson. The global existence problem in general relativity. In P.T. Chruściel and H. Friedrich, editors, *The Einstein Equations and the Large Scale Behavior of Gravitational Fields: 50 Years of the Cauchy Problem in General Relativity*, pages 71–120. Birkhäuser, Basel, Switzerland; Boston, U.S.A., 2004.
- [3] L. Andersson and G.J. Galloway. dS/CFT and spacetime topology. *Adv. Theor. Math. Phys.*, 6:307–327, 2002, hep-th/0202161.
- [4] J. Arms and J. Marsden. The absence of Killing fields is necessary for linearization stability of Einstein's equations. *Indiana Univ. Math. J.*, 28:119–125, 1979.
- [5] V.A. Belinskii, I.M. Khalatnikov, and E.M. Lifshitz. Oscillatory approach to a singular point in the relativistic cosmology. *Adv. Phys.*, 19:525–573, 1970.
- [6] V.A. Belinskii, I.M. Khalatnikov, and E.M. Lifshitz. A general solution of the Einstein equations with a time singularity. *Adv. Phys.*, 31:639–667, 1982.
- [7] F. Beyer. *Asymptotics and singularities in cosmological models with positive cosmological constant*. PhD thesis, Max Planck Institute for Gravitational Physics, 2007, gr-qc/0710.4297.
- [8] F. Beyer, 2008. Private communication with M.T. Anderson.
- [9] F. Beyer. A numerical approach for hyperbolic problems with spatial \mathbb{S}^3 -topology. preprint, 2008, arXiv:0804.4222 [gr-qc].
- [10] J.P. Boyd. *Chebyshev and Fourier Spectral Methods*. Dover Publications, Inc., 2nd edition, 2001.
- [11] D. Brill and F. Flaherty. Maximizing properties of extremal surfaces in general relativity. *Annales de L'Institut Henri Poincare Section Physique Theorique*, 28:335–347, May 1978.
- [12] P. Chruściel, J. Isenberg, and V. Moncrief. Strong cosmic censorship in polarized Gowdy spacetimes. *Class. Quant. Grav.*, 7:1671–1680, 1990.
- [13] P.T. Chruściel. On space-times with $U(1) \times U(1)$ symmetric compact Cauchy surfaces. *Annals Phys.*, 202:100–150, 1990.
- [14] P.T. Chruściel and J. Isenberg. Nonisometric vacuum extensions of vacuum maximal globally hyperbolic spacetimes. *Phys. Rev. D*, 48(4):1616–1628, Aug 1993.
- [15] J.W. Cooley and J.W. Tukey. An algorithm for the machine calculation of complex Fourier series. *Math. Comput.*, 19:297–301, 1965.
- [16] H. Friedrich. Existence and structure of past asymptotically simple solutions of Einstein's field equations with positive cosmological constant. *J. Geom. Phys.*, 3(1):101–117, 1986.
- [17] H. Friedrich. On the existence of n -geodesically complete or future complete solutions of Einstein's field equations with smooth asymptotic structure. *Commun. Math. Phys.*, 107:587–609, 1986.

- [18] H. Friedrich. Einstein equations and conformal structure: Existence of anti-De Sitter-type spacetimes. *J. Geom. Phys.*, 17:125–184, 1995.
- [19] H. Friedrich. *The Conformal Structure of Spacetime: Geometry, Analysis, Numerics*, chapter "Conformal Einstein Evolution". Lecture Notes in Physics. Springer, 2002.
- [20] H. Friedrich and G. Nagy. The initial boundary value problem for Einstein's vacuum field equations. *Commun. Math. Phys.*, 201:619–655, 1999.
- [21] H. Friedrich, I. Racz, and R.M. Wald. On the rigidity theorem for spacetimes with a stationary event horizon or a compact Cauchy horizon. *Commun. Math. Phys.*, 204:691–707, 1999, gr-qc/9811021.
- [22] H. Friedrich and B. G. Schmidt. Conformal geodesics in general relativity. *Proc. Roy. Soc. Lond. A*, 414:171–195, 1987.
- [23] M. Frigo and S.G. Johnson. FFTW Library, <http://www.fftw.org/>.
- [24] D. Garfinkle. Numerical simulations of Gowdy spacetimes on $S^2 \times S^1 \times R$. *Phys. Rev. D*, 60(10):104010, Oct 1999, gr-qc/9906019.
- [25] R.H. Gowdy. Vacuum space-times with two parameter spacelike isometry groups and compact invariant hypersurfaces: Topologies and boundary conditions. *Ann. Phys.*, 83:203–241, 1974.
- [26] S.W. Hawking and G.F.R. Ellis. *The large scale structure of space-time*. Cambridge University Press, 1973.
- [27] S.W. Hawking and I.L. Moss. Supercooled phase transitions in the very early universe. *Phys. Lett. B*, 110(1):35–38, 1982.
- [28] Intel. Intel Fortran Compiler, <http://www.intel.com/support/performance/tools/>.
- [29] J. Isenberg and V. Moncrief. Asymptotic behavior of the gravitational field and the nature of singularities in Gowdy space-times. *Ann. Phys.*, 199:84–122, 1990.
- [30] E.M. Lifshitz and I.M. Khalatnikov. Investigations in relativistic cosmology. *Adv. Phys.*, 12:185–249, 1963.
- [31] V. Moncrief. The space of (generalized) Taub-NUT spacetimes. *J. Geom. Phys.*, 1(1):107–130, 1984.
- [32] V. Moncrief and J. Isenberg. Symmetries of cosmological Cauchy horizons. *Commun. Math. Phys.*, 89:387–413, 1983.
- [33] E. Newman, L. Tamburino, and T. Unti. Empty-space generalization of the Schwarzschild metric. *J. Math. Phys.*, 4(7):915–923, 1963.
- [34] R. Penrose. Asymptotic properties of fields and space-time. *PRL*, 10:66–68, 1963.
- [35] R. Penrose. Gravitational collapse: The role of general relativity. *Riv. Nuovo Cim.*, 1:252–276, 1969.
- [36] R. Penrose. Singularities and time-asymmetry. In S.W. Hawking and W. Israel, editors, *General Relativity – An Einstein Centenary Survey*. Cambridge University Press, 1979.
- [37] R. Penrose and W. Rindler. *Spinors and Space-Time*, volume 1. Cambridge University Press, 1986.
- [38] W.H. Press, S.A. Teukolsky, W.T. Vetterlin, and B.P. Flannery. *Numerical Recipes in C*. Cambridge University Press, 2nd edition, 1999.
- [39] A.D. Rendall. Theorems on existence and global dynamics for the Einstein equations. *Living Reviews in Relativity*, 8(6), 2005, lrr-2005-6.
- [40] H. Ringström. Curvature blow up in Bianchi VIII and IX vacuum spacetimes. *Class. Quant. Grav.*, 17:713–731, 2000, gr-qc/9911115.
- [41] H. Ringström. Existence of an asymptotic velocity and implications for the asymptotic behavior in the direction of the singularity in T^3 -Gowdy. *Comm. Pure Appl. Math.*, 59(7):977–1041, 2006.
- [42] H. Ringström. Strong cosmic censorship in T^3 -Gowdy spacetimes. preprint, accepted in *Ann. of Math.*, 2006, <http://www.math.kth.se/~hansr/>.
- [43] A.G. Sanchez and C.M. Baugh. Cosmological parameters 2006. preprint, 2006, astro-ph/0612743.
- [44] D. N. Spergel et al. Three-year Wilkinson Microwave Anisotropy Probe (WMAP) observations: Implications for cosmology. *Astroph. J. Suppl. S.*, 170(2):377–408, 2007, astro-ph/0603449.
- [45] F. Ståhl. Fuchsian analysis of $S^2 \times S^1$ and S^3 Gowdy spacetimes. *Class. Quant. Grav.*, 19:4483–4504, 2002, gr-qc/0109011.
- [46] A. H. Taub. Empty space-times admitting a three parameter group of motions. *Annals of Mathematics*, 53(3):472–490, May 1951.